A Practical Look at Creep and Shrinkage in Bridge Design

Monte J. Smith, PE
Project Engineer
Arvid Grant and Associates
Olympia, Washington

David Goodyear, PE
Consulting Engineer
Olympia, Washington
(formerly Senior Engineer with
Arvid Grant and Associates)

Research has produced two major procedures for assessing creep and shrinkage; the ACI 209 method[1] and the CEB-FIP method.[2] Laboratory research into concrete creep and shrinkage has been conducted for decades, and excellent analytical procedures for evaluating structures for creep and shrinkage have been presented in the literature.[3-5]

Creep and shrinkage are factors in the design of a variety of bridge details. (The focus here will be on creep, for its treatment is somewhat more involved than that of shrinkage. However, the conclusions apply to both as elements of time dependent deformations.) Creep affects the setting of bearings and the size of sliding plates or laminated bearing pads, it affects the size and setting of expansion joints, and it affects the amount of girder shortening due to prestress and the corresponding loss of prestress, thereby also affecting the secondary moments in a prestressed girder bridge. The amount and character of creep influences the redistribution of forces in certain structures where the statical system changes during construction, and can, therefore, play a major role in stress distribution for composite construction.

Creep must be considered in the context of the entire design. The major effects of creep in concrete bridge structures can be summarized in three categories:

— Camber and deflection
— Prestress loss
— Stress redistribution

Where stress and strength is concerned, it is general practice to base engineering design on a conservative upper bound of demand, not on average demand. However, with creep we have an interest in both. Camber and deflection control for a free cantilever bridge does not have a high or low bias — we simply want to have the greatest chance of meeting the predicted values. Regarding stress redistribution due to free cantilever construction, we want to have confidence that we provide section capacity (for stress design) in excess of the future demands on the section — a more traditional design objective.

Clearly, no matter how precise the calculation method, the probability of achieving both objectives with one "average" creep coefficient is very low indeed. Even in the case of camber computations where mean values are appropriate, there are generally well-defined consequences for "missing" the target camber. The practical options for geometry correction can best be evaluated by inspecting a range of creep coefficients, rather than by a refinement of analytical procedures.

Material Behavior

Branson[6] lists the following parameters as affecting creep or shrinkage strains in concrete:

- Member size
- Water-cement ratio
- Mix proportions
- Aggregate type
- Length of curing
- Curing temperature
- Curing humidity
- Environmental temperature
- Time of initial loading
- Duration of load
- Number of load cycles
- Unloading period
- Stress distribution
- Stress magnitude
- Stress rate

Some of these factors are more variable than others, but certainly few of these factors can be taken as deterministic — especially in the design stage of a project.

To look at the variability and uncertainty in time dependent deformations we will look at three major parameters — the (pseudo) elastic modulus, the creep coefficient, and the loading history. Each plays a major role in both the ACI and the CEB-FIP methods for determining creep effects.

Material research presented by Nilson[7] and Branson et al.[8] is typical of the data available on concrete modulus and creep coefficient. These particular data

Synopsis

Computations for creep and shrinkage affect a variety of details in concrete bridge structures. From the size of expansion joints and bearings to the amount of prestress loss and long term deflection, creep and shrinkage in concrete can either govern or greatly influence final design details and construction of our modern bridges.

In current practice, the treatment of creep and shrinkage is handled differently than other loads. While we strive to design our bridges for the maximum demands of live loads, dead loads, temperature and other parameters, we have consistently chosen to look at average demand due to creep and shrinkage.

This paper presents the viewpoint that the large degree of variability in both concrete properties and method of design justifies a change from our deterministic approach to design for creep and shrinkage to one that accommodates the variability in concrete properties. Because it is a more complex time dependent strain than shrinkage, the focus of this paper is on creep.

The current state of the art in analysis of creep effects is reviewed, with ACI and CEB-FIP type analyses related to the real world difficulties in modern bridge design.

Table 1. East Huntington field elastic moduli tests.

Test Number	f'_c psi	$E \times 10^6$ psi	$E/\sqrt{f'_c}$
1	11300.00	5.05	47506.40
2	10600.00	5.30	51478.15
3	10600.00	5.04	48952.81
4	10600.00	5.10	49535.58
5	12400.00	5.30	47595.41
6	10600.00	5.54	53809.24
7	10600.00	5.40	52449.44
8	12100.00	5.30	48181.82
9	10800.00	4.82	46380.47
10	10950.00	4.42	42239.15
11	11500.00	5.32	49609.26
12	11600.00	5.33	49487.81
13	11700.00	5.30	48998.52
14	11800.00	5.31	48882.51
15	10400.00	4.40	43145.55
16	9900.00	4.43	44523.18
17	10600.00	4.81	46718.85
18	11000.00	5.20	49580.05
19	11300.00	5.30	49858.21
20	11500.00	5.06	47184.74
21	11300.00	5.05	47506.40
22	11800.00	5.30	48790.45
23	12100.00	5.30	48181.82
24	10900.00	4.45	42623.27
25	10400.00	5.15	50499.90
26	11500.00	5.04	46998.24
27	11400.00	5.03	47110.27
			Mean = 48067.68
			Standard deviation = 2676.23

yield coefficients of variation in the range of 0.15 for modulus (expressed as $E/\sqrt{f'_c}$) and 0.3 for creep coefficient. In comparing the data with both ACI and CEB-FIP procedures, Bazant[9,10] finds that both ACI and CEB-FIP yield coefficients of variation for creep between test data and predicted values of about 0.3, which is in agreement with the previously mentioned data.

While project specific testing can certainly help to narrow the range of these variables, such testing at the design stage will not eliminate the characteristic variability in concrete properties. The East Huntington Bridge project is a good example of this point. A state of the art material testing program during the design phase indicated that the modulus of the laboratory mix was approximately 6,500,000 psi (44850 MPa). The construction contract called for field testing of concrete and the results of that testing are indicated in Table 1. The most noteworthy point is that, while the variation across the sample was fairly low, the mean value for modulus was approximately 20 percent below that determined for design using project specific testing.

Creep coefficients were also determined for the East Huntington project. Of necessity, any such testing must be of short duration, and prediction methods must be used to extrapolate the creep data to obtain total creep coefficients. Figs. 1 through 4 show results from this job specific testing. Creep results were obtained for loading ages of 14, 28, 90 and 365 days. Tests were run for a loading duration of one year. Plotted along with the results are both the ACI 209 and CEB-FIP Code projections for these cases.

For designers considering creep behavior of concrete, these figures illustrate several important characteristics:

First, the scatter among the tests is very large. The authors are aware of other major construction projects in which the high and low creep coefficients determined during construction varied by as much as 100 percent.

Second, the CEB-FIP method generally indicates higher creep than does the ACI method. However, all ACI projections shown are based on the "average" ultimate creep coefficient of 2.35, pointing to a major shortcoming (or misunderstanding) in the ACI guidelines — there is no such thing as an "average" creep coefficient. A more definitive guideline is needed in ACI 209 for estimating creep coefficients for design.

Fig. 5 shows the difference between the ACI 209 and CEB-FIP methods for the 14-day loading age case with the ultimate creep coefficients normalized to the same value. The graph clearly shows what the authors have found to be a significant difference between the two codes, and that is the curvature (or rate) of the creep curve — ACI creep burns out faster than CEB-FIP. This difference can have a significant effect on the analytical results for certain construction sequences that involve changes to the statical system.

A third observation is that the trend of the loading age correction factor in the ACI method for late loading ages (one year in this case) is to cause an apparent increase in creep, and a reversal of position with CEB-FIP provisions in terms of magnitude of creep.

Code Procedures

The ACI and CEB-FIP methods are both empirical. Rather than being based on development of a theoretical material model, they are expressions of numerical correlations with test data. While the format and standard correction factors for the two methods differ, the primary difference is that the CEB-FIP provisions address creep recovery (rebound of the concrete after unloading) separately from creep development. This difference leads to a two component creep model for the CEB-FIP method, with one component representing the recoverable portion of creep and another representing the irrecoverable component.

In the development of creep under load, the similarities between the two methods are more significant than the differences. Both methods subscribe to the principle of superposition, i.e., the thesis that the total creep effect from multiple loads is a linear superposition of the individual effects from each load. Therefore, creep development for both methods depends not on total load, but on load history.

For a single component creep model like the ACI method, this means that (with correction for loading age, etc.,) the total creep is the sum of the creep for each load, based on each load duration. For a two component creep model like the CEB-FIP method, this means that the total creep is the sum of the recoverable and the irrecoverable creep for each load based on each load duration, and the total creep recovery is the sum of the recoveries for each load removed, according to each load history.

Fig. 6 shows a comparison of creep deformation computed by both ACI and CEB-FIP methods for a free cantilever under a concentrated load. Prior to unloading, the two methods agree quite well. After unloading, divergence develops due to the limited recoverable creep developed in the CEB-FIP

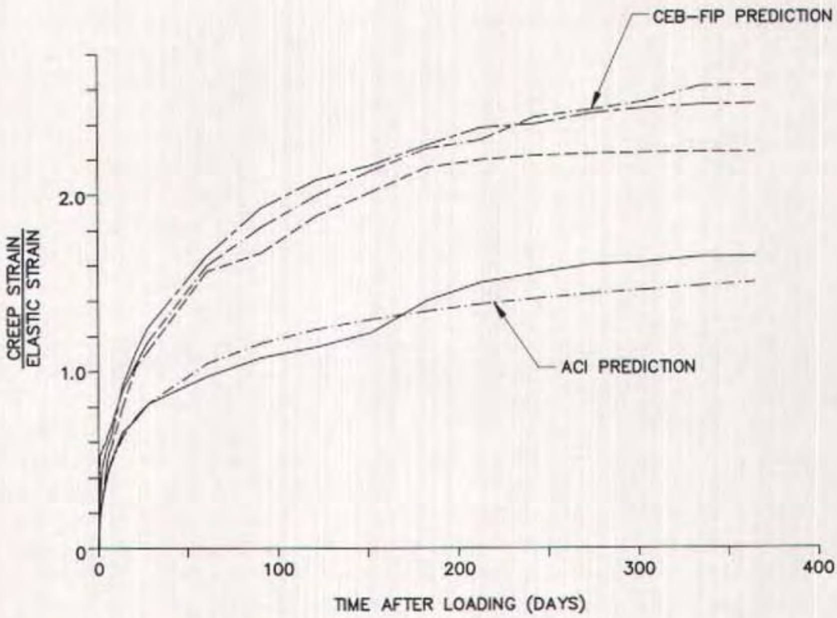

Fig. 1. Creep test results for 14-day age at loading.

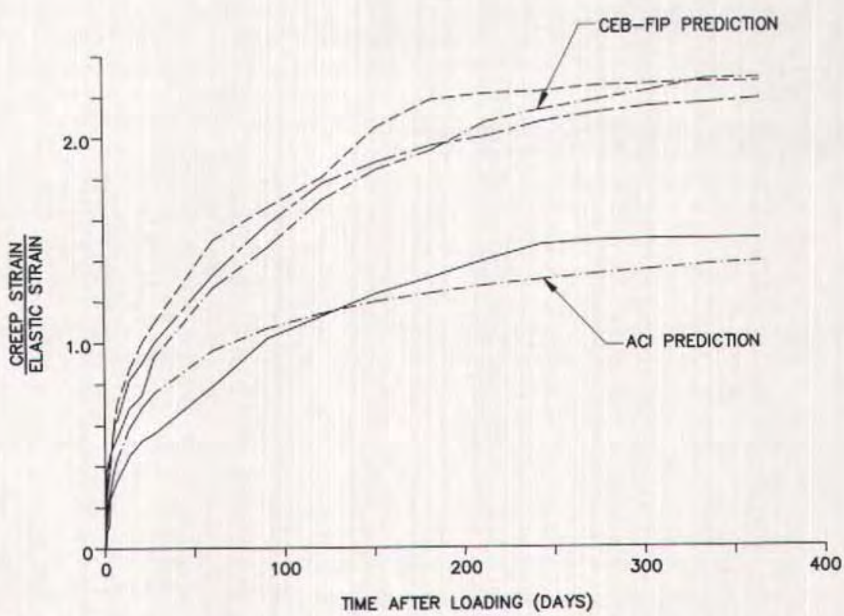

Fig. 2. Creep test results for 28-day age at loading.

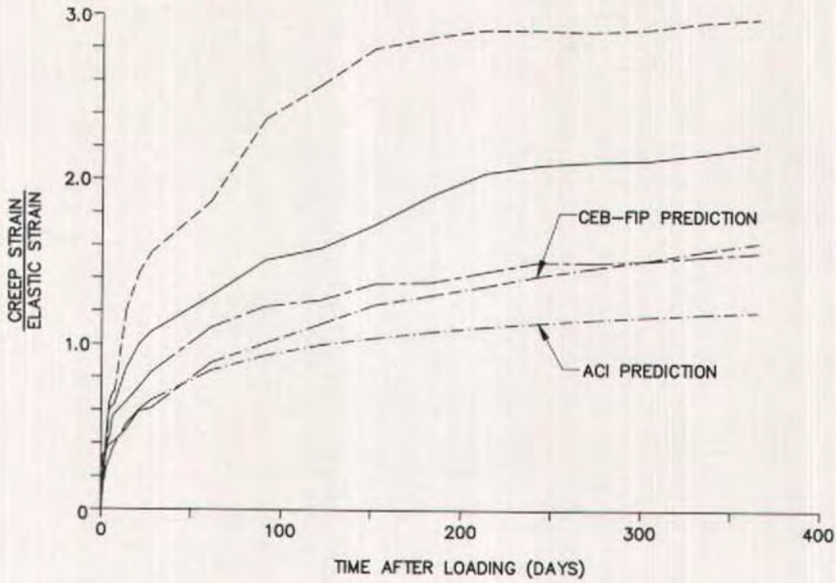

Fig. 3. Creep test results for 90-day age at loading.

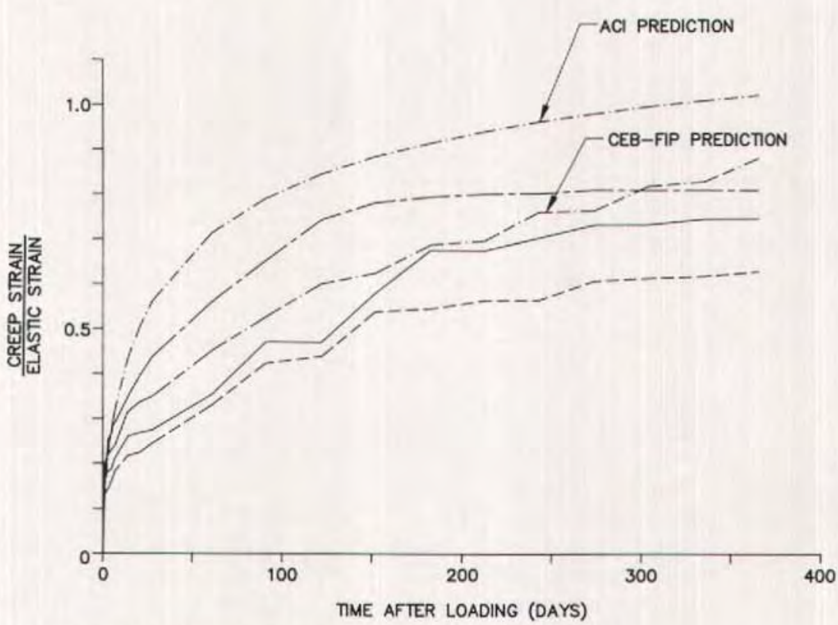

Fig. 4. Creep test results for 365-day age at loading.

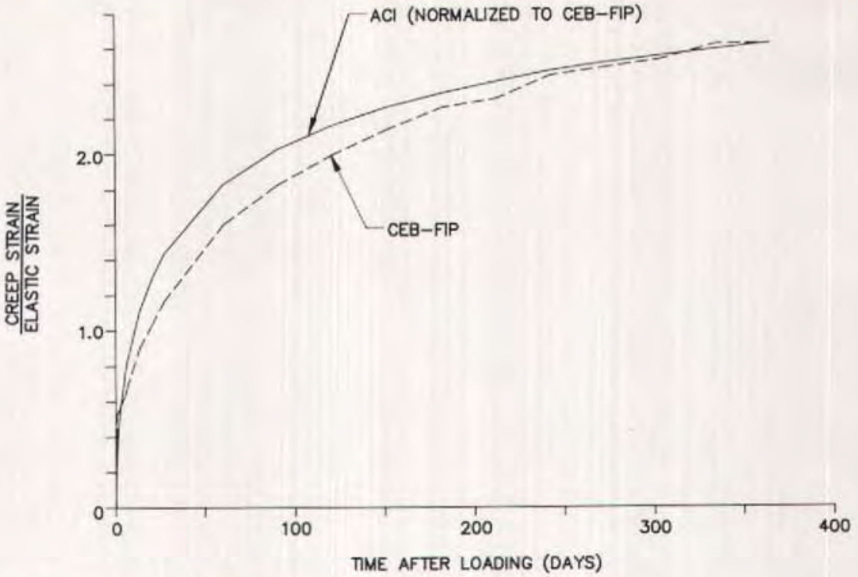

Fig. 5. ACI and CEB-FIP comparison (14-day age at loading).

model. The same initial elastic modulus and total creep coefficient was chosen for each method in this example. Clearly, a variation in creep coefficient of 25 to 30 percent would result in wide overlap of the results using either method.

Current Methods and Load History

The two component creep model described in the CEB-FIP Code is a generally accepted model for concrete cylinders subjected to discernable loading and unloading. However, the loading conditions in bridge structures are not as straight forward as the controlled load on a concrete cylinder. The time dependent analysis of modern concrete bridge structures involves changing loads on varying statical systems, accumulated changes in construction loading, and major stress reversals due to erection operations and continuity conditions. The loading history, even if it were retained, is obscure at best; and the definition of load as loading or unloading is equally obscure.

Most modern analysis codes that deal with creep utilize the so-called "target creep" method,[11-15] in which creep strain is described with a Dirichlet series, and the creep history is carried in a state variable, $A_{i,j}$, as described below:

$$\Delta \epsilon = \sum_i A_{i,j} \left\{ 1 - e^{-\lambda_i \Delta t_j} \right\}$$

$$A_{i,j} = A_{i,j-1} e^{-\lambda_i \Delta t_{j-1}} + \frac{\Delta \sigma}{E_c} a_i(\tau)$$

where

$\Delta \epsilon$ = incremental creep strain
$A_{i,j}$ = state variable containing accumulated creep history
$\Delta \sigma$ = increment of stress
Δt_j = current time interval
Δt_{j-1} = previous time interval
τ = current concrete age (for flow creep in CEB-FIP method)
a_i, λ_i = curve fitting coefficients
E_c = concrete modulus of elasticity

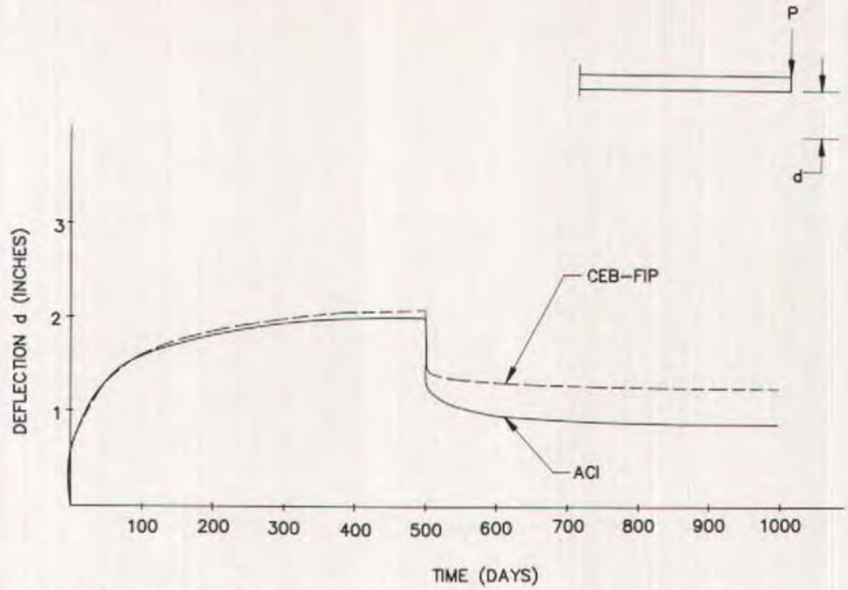

Fig. 6. Comparison of cantilever deflections by ACI and CEB-FIP methods.

The key to this method is that the loading history does not have to be carried along in the analysis because it is already stored in the state variable. The state variable reflects the accumulation of strain increments throughout the loading history and decays according to a numerical prescription to the total creep due to all stress increments applied on an element.

The curve fitting coefficients can be derived from the ACI method for a single component creep method, from the CEB-FIP provisions for a two component (two state variables) creep method, or from test results. The latter is preferable once mix designs have been established.

Because load history is not carried in the analysis, unloading is treated as loading with opposite sign. This creates complications for both target creep methods (single component and two component). The curve fitting coefficients provide for a fairly representative model of the ACI and CEB-FIP creep curves for applied loading. However, the state variables that are incremented with each load application retain the effects of each load for the remainder of the analysis. While in both the ACI and CEB-FIP methods creep development ceases with the removal of a load, in the target creep method the creep continues due to the inclusion of the initial load in the decaying state variable.

In addition, for the CEB-FIP method the amount of creep recovery for loads of short duration depends on the length of time the load has been acting. Since load history is not carried in the target creep analysis, this information is not available. Artificial corrections based on the sign of incremental creep strain in the target creep method to accommodate creep recovery make intuitive sense, but they are not an application of the empirical base of the CEB-FIP method, for they imply that creep recovery is independent of the initial load.

The practical result of the target creep method is that for an ACI type target creep model subject to unloading, the target is overestimated. But since the

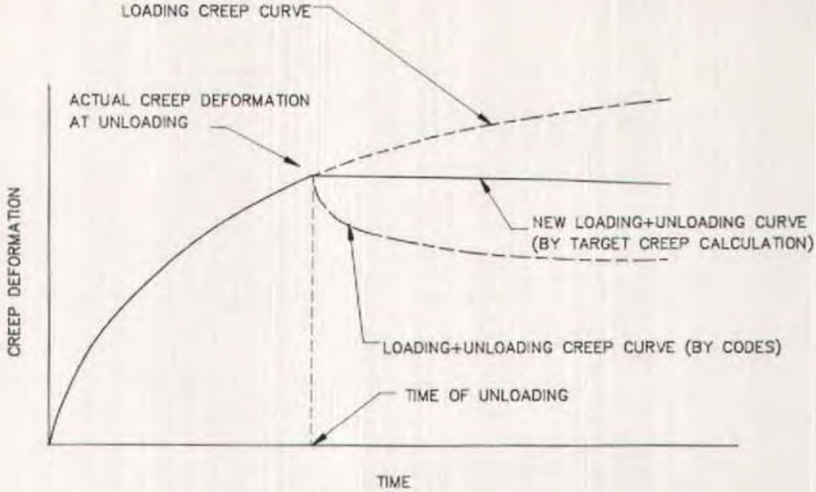

Fig. 7. Superposition of creep loading and unloading.

ACI method overestimates recovery, so is the recovery component. In contrast, the CEB-FIP type target creep model subject to unloading also includes an overestimate for the target, but will have a greatly reduced recovery component. Fig. 7 illustrates this process.

In effect, neither of the two popular code methods for creep and shinkage address the constantly changing loading conditions in a modern concrete bridge. And even if our analytical methods were perfect, we would still deal with substantial variability in material coefficients, leaving our results variable as well.

Case Study

Fig. 8 shows a simple three span cast-in-place segmental structure that will serve to illustrate the practical significance of creep behavior on segmental bridges.

Fig. 9 shows the erection sequence of the segments. The post-tensioning *P-e* diagram is shown in Fig. 10.

The bridge was evaluated using a time dependent analysis program that utilized a single component target creep method for concrete members. Curve fitting coefficients were developed for both an ACI 209 standard creep curve and for a flatter, CEB-FIP type curve represented by the majority of East Huntington tests shown in Figs. 1 through 4.

To evaluate the influence of the inevitably large variation on creep coefficient, the analysis was made by using coefficients for an ACI type curve, but varying the ultimate creep coefficient (C_u) from 2.35 to 4.36 (the former is the ACI "average" value, the latter is a total coefficient from the CEB-FIP Code for dry conditions). Fig. 11 shows the range in final dead load moment diagrams due to the variation in ACI type creep coefficient from 2.35 to 4.36. Figs. 12 and 13 show the final stresses in the bridge due to the variation in creep coefficient. Fig. 13 shows the difference in bottom flange stresses at midspan to be approximately 200 psi (1.38 MPa).

However, of greater significance is the third analysis for a creep coefficient of 3.35 (the average of the above two values). This analysis was carried out using the curve fitting coefficients for an ACI type curve as well as those for the

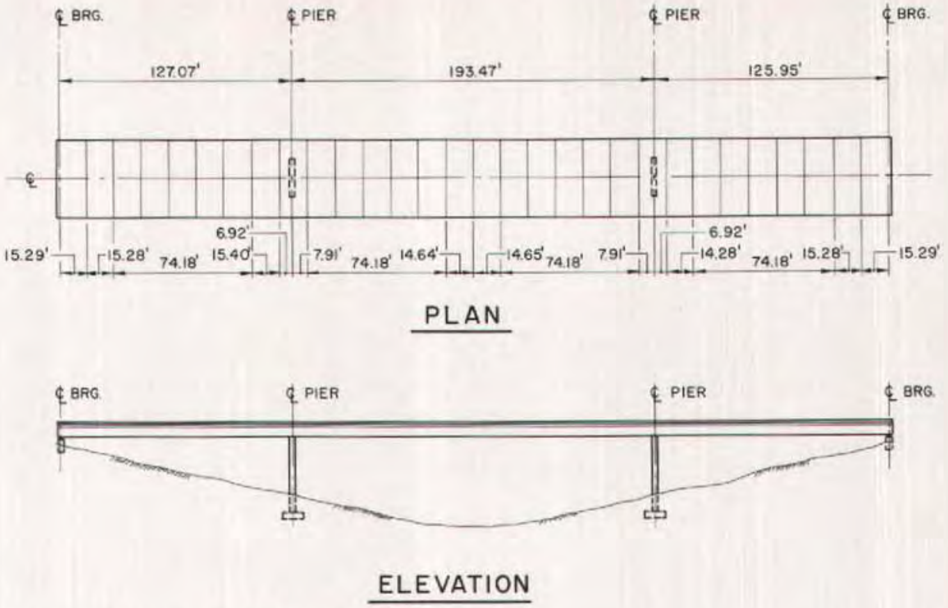

Fig. 8. Plan and elevation of case study.

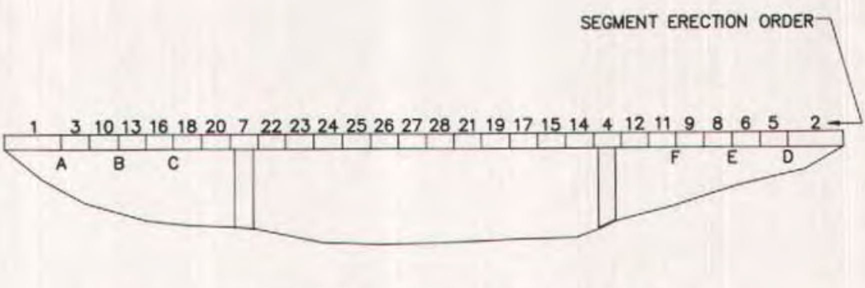

NOTE: LETTERS DENOTE TEMPORARY SUPPORTS DURING ERECTION.

Fig. 9. Case study erection sequence.

East Huntington data that resembled the CEB-FIP type curve (Fig. 14). While the increase in bottom flange tension for the ACI type curve in going from C_u = 2.35 to 3.35 is only 78 psi (0.54 MPa), the increase when using the flatter creep curve from the East Huntington data was 172 psi (1.19 MPa). Thus, this flatter curve, which leaves more creep strain until after main span closure, results in almost as much stress change as twice the increase in creep coefficient when using the steeper ACI creep curve.

The actual numbers presented here serve only for illustration. The important point is that, despite all the elaborate computation methods available today, the final stress state in a concrete bridge structure depends on the time dependent response of highly variable concrete material.

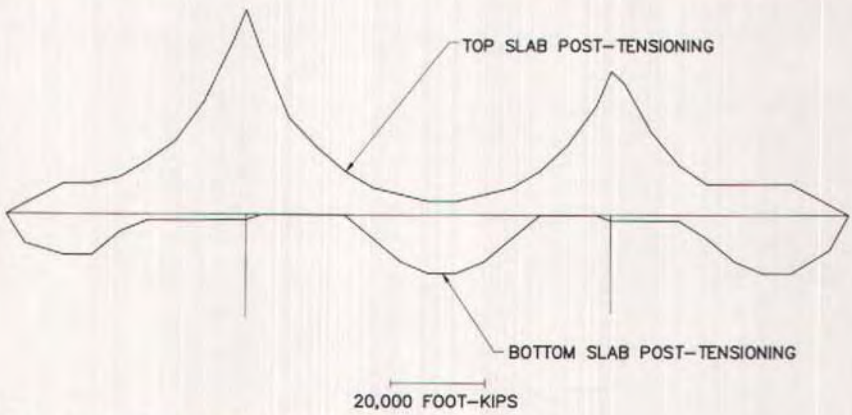

Fig. 10. Example post-tensioning *P-e* diagram.

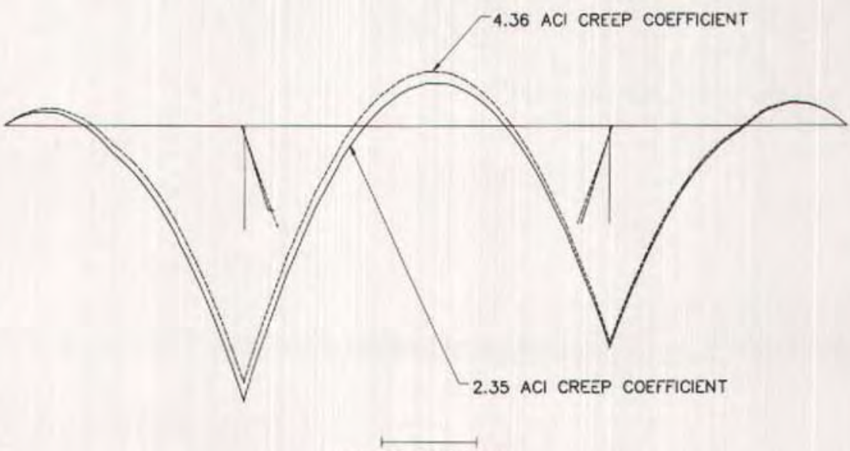

Fig. 11. Example moment diagrams.

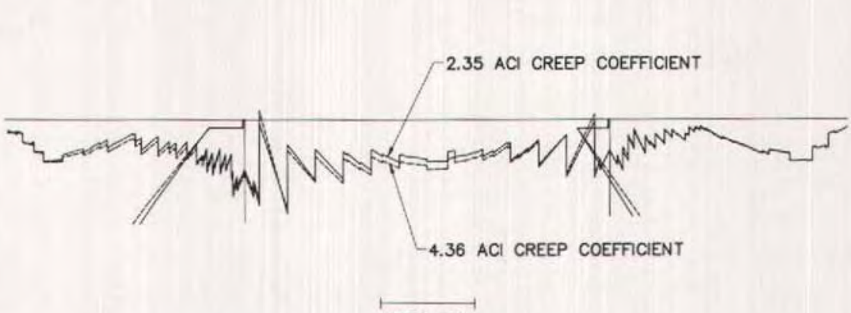

Fig. 12. Example top flange stress diagram.

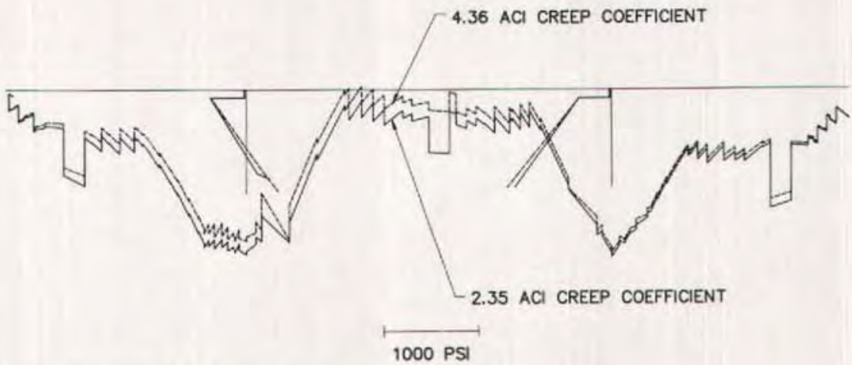

Fig. 13. Example bottom flange stress diagram.

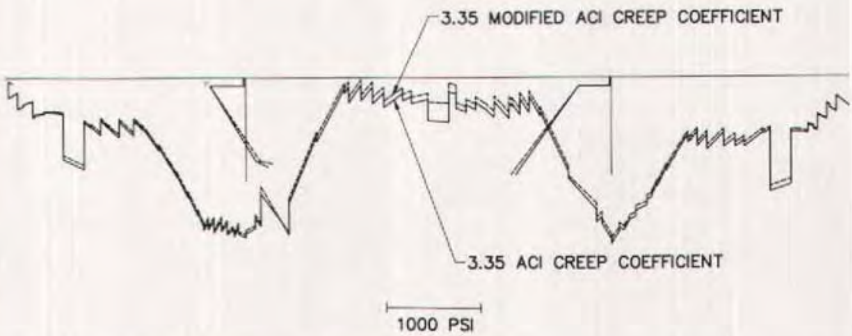

Fig. 14. Example bottom slab stress comparison.

Practical Design

The question remains; given the variable character of concrete material constants and the various influences of material behavior on design, what should we do in design? The following are some practical guidelines.

• **Use upper bound material constants for design.** We have two objectives in most designs involving creep and shrinkage. First, we want a safe design that satisfies serviceability requirements. Second, where segmental construction is concerned, we want to develop a construction procedure that will facilitate closure connections during construction.

Both conditions will not be met with one creep coefficient. Creep and shrinkage coefficients chosen for design should be upper bound values — values with less than a 5 percent chance of being exceeded in the field. Creep and shrinkage coefficients chosen for construction may be averages (averages are often used now for both design and construction) that can be determined from statistical evaluations of actual job mix designs. These values will give the greatest chance of hitting target geometry during construction.

- **Make designs insensitive to creep and shrinkage.** A good design should not be limited by a certain creep or shrinkage coefficient. High, and where appropriate, low values of creep coefficient should be tested to see that designs are viable within a broad range of material response. By employing balanced prestressing for dead load stages, continuous spans of prestressed concrete often can be designed so that creep effects on continuity stresses are small. Precasting greatly reduces the effects of creep and shrinkage on the final structure.

Continuous mild reinforcing steel is the best guard against shrinkage cracking, and it provides the ductility to redistribute stresses that may exceed those assumed in design. Mild steel bridges the gap between the ultimate strength conditions and service conditions, for often problems due to creep and shrinkage occur at the service stage in structures that are nominally adequate for ultimate load conditions. Mild steel should be included wherever possible to provide ductility in prestressed concrete members. One-half of one percent of the flange area is suggested as a guide.[16]

- **Use judgment with analysis.** Do not get carried away with the numbers — your input is good to two significant figures. Do not try to stretch your analysis to hundredths of an inch. Use simple hand checks such as those in the Post-Tensioning Institute Manual[17] as an aid in assessing results.

Muller and Podolny[18] review an appropriate example, the Houston Ship Channel Bridge, in their book on segmental bridges. The text shows an approximate analysis for continuity moment (similar to the method in Ref. 17) and compares it to the more exhaustive computer solution. The answers differ by less than 10 percent; that is excellent agreement for this work.

Conclusion

What we have today are two popular, often competing methods for creep and shrinkage prediction. However, neither of these two methods fits the practical demands of general bridge design.

The target creep method was developed over a decade ago and stands as the first step in the advance toward a practical design tool for evaluating creep in bridges. Unfortunately, the second necessary step, namely, supporting material research and code guidelines, have not matched the advance in analytical capabilities.

What we need today must come from both material research laboratories and design practice. We need physical material models that reflect the constant fluctuation of stress in concrete; models that enable a design engineer to isolate the stress regime on an element rather than fabricate artificial scenarios of load history. And we need organized, consistent data upon which to build a statistically significant data base.

All major concrete bridge projects should include provisions for systematic measurement of geometry during construction and into service. These data should be filed in a public bank, readily accessible for both practitioners and researchers. With an increasing data base available to code writers, future guidelines should be cast in probabilistic terms, offering the designer a means of establishing a reliability based design for creep and shrinkage.

REFERENCES

1. ACI Committee 209, "Prediction of Creep, Shrinkage and Temperature Effects in Concrete Structures," Special Publication SP-76, *Designing for Creep and Shrinkage in Concrete Structures*, American Concrete Institute, Detroit, Michigan, pp. 193-300.
2. *CEB-FIP Model Code for Concrete Structures*, Comité Euro-International du Béton (CEB), 1978. Available from Fédération Internationale de la Précontrainte, 11 Upper Belgrave Street, London SW1X 8BH, England.
3. Tadros, M. K., Ghali, A., and Dilger, W. H., "Time Dependent Analysis of Composite Frames," *Journal of the Structural Division, ASCE*, V. 103, No. ST4, April 1977, pp. 871-884.
4. Dilger, W. H., "Creep Analysis of Prestressed Concrete Structures Using Creep-Transformed Section Properties," PCI JOURNAL, V. 27, No. 1, January-February 1982, pp. 98-118.
5. Tadros, M. K., Ghali, A., and Dilger, W. H., "Long-Term Stresses and Deformation of Segmental Bridges," PCI JOURNAL, V. 24, No. 4, July-August 1979, pp. 66-87.
6. Branson, D. E., *Deformations of Concrete Structures*, McGraw Hill, New York, N.Y., 1977, 546 pp.
7. Ngab, A. S., Nilson, A. H., and Slate, F. O., "Shrinkage and Creep of High Strength Concrete," *ACI Journal*, Proceedings V. 78, No. 4, July-August 1981, pp. 255-261.
8. Meyers, B. L., Branson, D. E., and Schumann, C. G., "Prediction of Creep and Shrinkage Behavior for Design from Short Term Tests," PCI JOURNAL, V. 17, No. 3, May-June 1972, pp. 29-45.
9. Bazant, Z. P., Chern, JC., "Log Double Power Law for Concrete Creep," *ACI Journal*, Proceedings V. 82, No. 5, September-October 1985, pp. 665-675.
10. Bazant, Z. P., Chern, JC., "Bayesian Statistical Prediction of Concrete Creep and Shrinkage," *ACI Journal*, Proceedings V. 81, No. 4, July-August 1984, pp. 319-330.
11. Khalil, M. S., "Time Dependent Nonlinear Analysis of Prestressed Concrete Cable Stayed Girders and Other Concrete Structures," University of Calgary, Alberta, Canada, 1979, 246 pp.
12. van Zyl, S. F., "Analysis of Segmentally Erected Prestressed Concrete Box Girder Bridges," *Report No. SESM 78-02*, University of California at Berkeley, January 1978, 265 pp.
13. Kabir, A. F., "Nonlinear Analysis of Reinforced Concrete Panels, Slabs and Shells for Time Dependent Effects," *Report No. SESM 76-06*, University of California at Berkeley, December 1976, 219 pp.
14. Bazant, Z. P., and Wu, S. T., "Dirichlet Series Creep Function for Aging Concrete," *Journal of the Engineering Mechanics Division, ASCE*, V. 99, No. EM2, April 1973, pp. 367-387.
15. Ketchum, M. A., "Redistribution of Stresses in Segmentally Erected Prestressed Concrete Bridges," *Report No. SESM 86-07*, University of California at Berkeley, May 1986, 185 pp.
16. Elbadry, M.; Ghali, A.; "Thermal Stresses and Cracking of Concrete Bridges," *ACI Journal*, Proceedings V. 83, No. 6, November-December 1986, pp. 1001-1009.
17. *Precast Segmental Box Girder Bridge Manual*, Post-Tensioning Institute, Phoenix, Arizona, 1978, 116 pp.
18. Podolny, W., and Muller, J. M., *Construction and Design of Prestressed Concrete Segmental Bridges*, John Wiley & Sons, New York, N.Y., 1982, 561 pp.

* * *

NOTE: Discussion of this article is invited. Please submit your comments to PCI Headquarters by February 1, 1989.